JOURNAL OF COMPUTATIONAL PHYSICS 12, 153–170 (1973)

Solution by Characteristics at Fixed Time Interval of the Equations of One Dimensional Unsteady Flow

T. L. CHOW

California State College—Stanislais, Turlock, California 95380

Received January 18, 1972

The solution by characteristics at fixed time interval of the equations of one dimensional unsteady flow is presented in this paper. We determine the new points by initially fixing the time step and then use the fluid characteristic to determine the spatial location of the points at the next time level. The results of the propagation of a strong radiative shock into a density gradient for which the method was designed is also included.

I. INTRODUCTION

During a search for a possible origin of the high velocity neutral hydrogen gases at high galactic latitudes, we examined the consequences of high velocity gas collisions. After collision two strong radiative shocks appear and move away from the contact surface into gases 1 and 2, respectively (Fig. 1). Gas 2 is taken to be homogeneous, whereas, gas 1 is inhomogeneous.

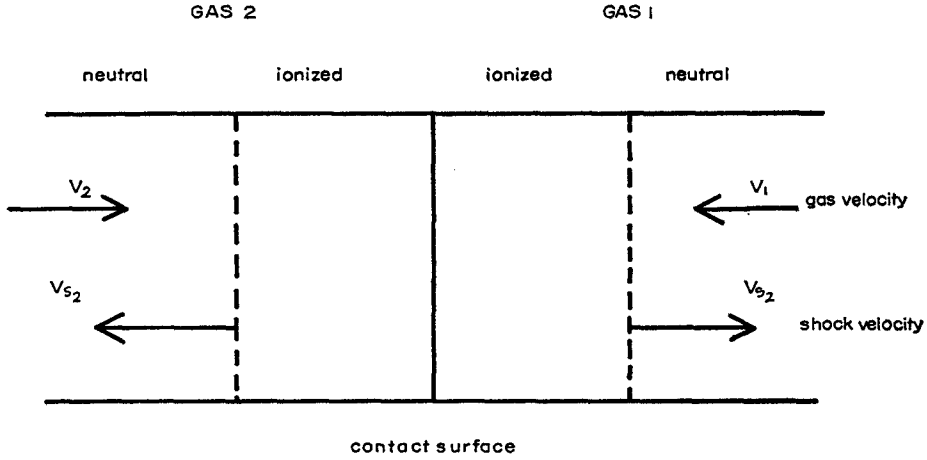

FIG. 1. Shocks in colliding gases.

In studying the shock propagation in inhomogeneous medium, the change in the flow pattern behind the shock fronts caused by cooling, the reflected compression waves from the fronts, etc., should be included in the treatment. So one has to solve the hydrodynamic equations. However, there is no exact analytical solution. In our description of two shocks created by colliding gas clouds, the most practical method was found to be the method of characteristics. It has certain advantages over the other methods, [4]. On the other hand, there is one disadvantage of the solution on a characteristic mesh. One has no control over the points at which the solution gets determined, and in general two dimensional interpolation in the characteristic mesh is required. In order to overcome this difficulty, we define mesh points in advance in both space and time and perform the interpolation as the calculation proceeds [3].This has the advantage that interpolations are always one dimensional.

II. The Equations of Motion in Characteristic Form

Using the method of Lagrange undetermined multipliers [2], we transform the equations of motion in standard from

equation of continuity $$\frac{D\rho}{Dt} + \rho \frac{\partial u}{\partial x} = 0, \tag{1}$$

equation of motion $$\rho \frac{Du}{Dt} + \frac{\partial P}{\partial x} = 0, \tag{2}$$

equation of energy conservation $$\rho \frac{D\epsilon}{Dt} - \frac{P}{\rho} \frac{D\rho}{Dt} = -Q, \tag{3}$$

where P, ρ, u are the gas pressure, gas density, and the fluid velocity,

$$\epsilon = \frac{1}{\gamma - 1} \frac{P}{\rho} + \frac{1}{2} V_i^2,$$

$\frac{1}{2}V_i^2$ is the ionization energy per gram and is taken as a constant, Q is the energy loss per unit volume and per second, into characteristic-form:

$$dp + \gamma \frac{P}{c} du + (\gamma - 1)\, Q\, dt = 0, \tag{4a}$$

along

$$dx = (u + c)\, dt; \tag{4b}$$

$$dp - \gamma \frac{P}{c} du + (\gamma - 1)\, Q\, dt = 0, \tag{5a}$$

along

$$dx = (u - c)\, dt; \tag{5}$$

$$(1 - \gamma)\, dp + \frac{2\gamma p}{c}\, dc + (\gamma - 1)\, Q\, dt = 0, \tag{6a}$$

along

$$dx = u dt. \tag{6b}$$

In calculations, the characteristic equations are placed in finite difference form by replacing the differential coefficient by a difference ratio over the interval and replacing other quantities by the arithmetic mean over the interval.

III. Calculation by Characteristics at Fixed Time Intervals

As mentioned in the introduction, we define the mesh points in advance in both space and time and perform the interpolations as the calculation proceeds.

A. *Calculation of Ordinary Points*

Referring to Fig. 2, if we consider the conditions to be known at points A, B, S_0 on the base line, the determination of conditions at a new point P is relatively simple for a region containing no singularities. The point P to be found is formed

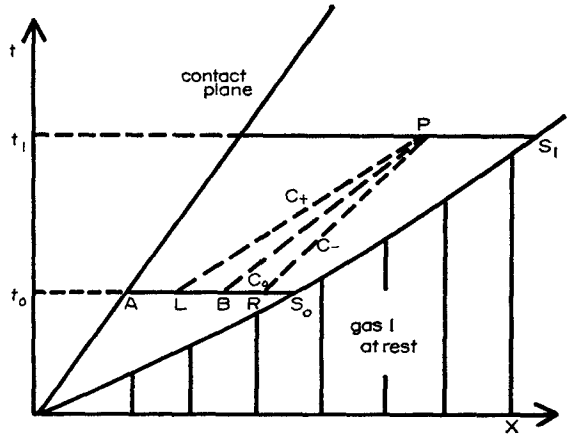

FIG. 2. Calculation of an ordinary point by characteristics. The shock 2 is the mirror image of the shock 1, so for shock 2, C_+ and C_-, and R and L are interchanged.

by intersection of a streamline through B with the new horizontal line $t_1 = t_0 + \Delta t$. The selection of the time interval Δt as the calculation proceeds will be discussed in Section E. We next trace back from P two characteristics. One meets the base line t_0 at L (the positive one), while the other intersects the line t_0 at R (the negative one). If M_A means the value of some variable M at the point A and $[M]_{AB}$ the average of the values at A and B, the equations to be solved may be written

$$(P_p - P_L) + \gamma \left[\frac{P}{c}\right]_{pL} (u_p - u_L) + (\gamma - 1)[Q]_{pL}\, \Delta t = 0, \tag{7a}$$

$$x_p - x_L = [u + c]_{pL}\, \Delta t, \tag{7b}$$

along pL;

$$(P_p - P_R) - \gamma \left[\frac{P}{c}\right]_{pR} (u_p - u_R) + (\gamma - 1)[Q]_{pR}\, \Delta t = 0, \tag{8a}$$

$$x_p - x_R = [u - c]_{pR}\, \Delta t, \tag{8b}$$

along pR; and

$$(1 - \gamma)(P_p - P_B) + 2\gamma \left[\frac{P}{c}\right]_{pB} (c_p - c_B) + (\gamma - 1)[Q]_{pB}\, \Delta t = 0, \tag{9a}$$

$$x_p - x_B = [u]_{pB}\, \Delta t, \tag{9b}$$

along pB.

The solution of these equations by an iterative method is quite straightforward if we assume values initially for the mean values in square brackets. For a first approximation it suffices to replace the mean values in square brackets by values appropriate to the initial point on the base line from which the characteristics are drawn. The accuracy of this procedure depends only on the magnitude of the time step used. Inaccuracies are introduced due to the fact that the characteristic curves have been replaced by short straight lines having appropriate slopes. These errors can be reduced by reducing the magnitude of the time step. The iteration proceeds as follows:

(1) Solve Eq. (9b) for x_p.

(2) In order to determine conditions at P, we first require values of the flow variables at L and R. We can obtain them by interpolation between the values at A, B, and S_0. We first solve the following four equations simultaneously for x_L, x_R, $(u + c)_L$, and $(u - c)_R$:

$$(u + c)_L = (u + c)_A \frac{x_L - x_B}{x_A - x_B} + (u + c)_B \frac{x_L - x_A}{x_B - x_A},$$

$$(u - c)_R = (u - c)_A \frac{x_R - x_B}{x_A - x_B} + (u - c)_B \frac{x_R - x_A}{x_B - x_A},$$

with Eqs. (7b) and (8b).

(3) Determine the flow variables (u, p, c) at L and R by interpolation between the values at A, B.

(4) Solve Eqs. (7a) and (8a) for u_p and P_p.

(5) Solve Eq. (9a) for c_p.

(6) The terms in square brackets may now be recalculated as the average of the values at the old point and the new point p, and the process repeated from (1) until x_p, u_p, P_p, and c_p remain uncyanged on iteration (accuracy $\approx 10^{-6}$). The number of iteration required for convergence in our problem for which the method was designed is about 7.

B. *Calculation of Shock Points*

Across a shock front all dependent variables are discontinuous. Since the shock velocity is a function of the other flow variables, the paths of shock waves have to be determined simultaneously with the calculation of the rest of the flow. The magnitude of the jumps in these variables are determined by solving the Rankine–Hugoniot relations which can be written as [8]

$$\rho/\rho' = \left[\gamma - \sqrt{1 + (\gamma^2 - 1)\left(\frac{V_i}{V_s}\right)^2}\right]\Big/(\gamma - 1), \tag{10a}$$

$$P' = \rho V_s^2(1 - \rho/\rho'), \tag{10b}$$

$$u' = V_s(1 - \rho/\rho'), \tag{10c}$$

where ρ = gas density in front of the shock front, a given function of x. These, together with an equation of state

$$P' = \frac{k\rho'}{\mu' H} T' \tag{11}$$

give four equations to solve for five unknowns, u', T', V_s, P', and ρ', assuming that conditions are known in front of the shock front. Thus, if one variable is assumed, we can solve for the other unknowns. In Eqs. (10a) to (11), all primed quantities refer to the post-schock gases, and μ' denotes the mean particle mass expressed in the units of the mass of proton.

Referring to Fig. 3 the shock path is represented by S_0S_1, the method of determining S_1 found to be most practical being the following:

(1) Obtain an estimate of the position of S_1 by assuming the value of shock velocity at S_1

$$x_{S_1} = x_{S_0} + \tfrac{1}{2}(S_0 + S_1)\,\Delta t.$$

The value of S_1 is initially assumed to be S_0.

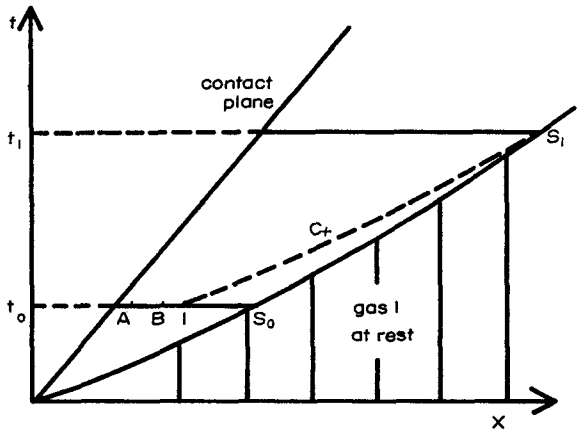

FIG. 3. Calculation of a shock point. S_0S_1 is the path of the shock.

(2) Solve Eq. (10a) for ρ/ρ'.

(3) Solve Eq. (10b) bor P'.

(4) Solve Eq. (10c) for u'.

(5) The gas density, ρ, in front of the shock is a given function of x. Substitution of ρ into (2) yields ρ', the shocked gas density behind the front.

(6) Construct a characteristic from S_1 to intersect the old base line ABS_0 at I, then

$$x_I = x_{S_1} - [u + c]_{S_1 I}\,\Delta t, \tag{12a}$$

$$\delta = P_{S_1} - P_I + \gamma\left[\frac{P}{c}\right]_{S_1 I}(u_{S_1} - u_I) + (\gamma - 1)[Q]_{S_1 I}\,\Delta t, \tag{12b}$$

where δ is a residual which will be zero when the true solution is determined, and $P_{S_1} = P'$, $u_{S_1} = u'$.

(7) Solve

$$(u + c)_I = (u + c)_B\frac{x_I - x_{S_0}}{x_B - x_{S_0}} + (u + c)_{S_0}\frac{x_I - x_B}{x_{S_0} - x_B}$$

together with Eq. (12a) for x_I.

(8) Determine the conditions at I by interpolation between the values at S_0 and B.

(9) Calculate δ from Eq. (12b). In general δ is a function of S_1, we adjust S_1 by iteration until the residual δ meets the requirement, say $|\delta|/P_{S_0} \ll 10^{-14}$. The

number of iteration for our problem is about 10. The pressure, particle velocity, etc. behind S_1 are calculated at each iteration as functions of S_1 by repeating from (1).

C. *Calculation at Contact Surface*

Referring to Fig. 4 the contact surface is represented by the point C_0 (at time t_0, say) which at the later time $t_1(=t_0 + \Delta t)$ has moved to C_1. Across a contact surface pressure and velocity are continuous, so the difference equations to be solved along C_1G are

$$P_{C_1} - P_G - \gamma \left[\frac{P}{c}\right]_{C_1G} (u_{C_1} - u_G) + (\gamma - 1)[Q]_{C_1G}\, \Delta t = 0, \tag{13a}$$

$$x_{C_1} - x_G = [u - c]_{C_1G}\, \Delta t; \tag{13b}$$

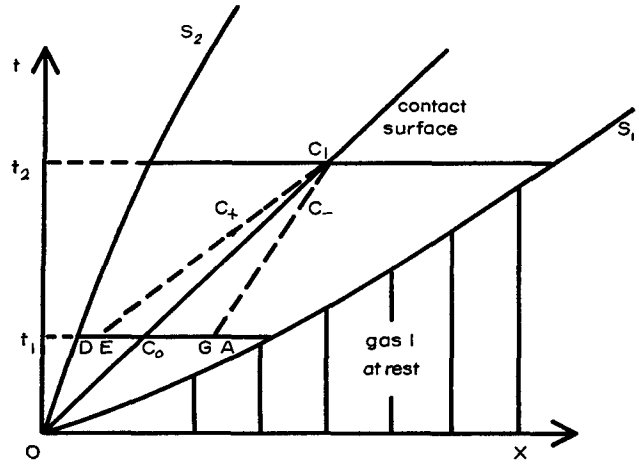

FIG. 4. Calculation at contact surface. OS_1 is the path of the shock,[1] OS_2 the path of the shock[2].

along C_1E are

$$P_{C_1} - P_E + \gamma \left[\frac{P}{c}\right]_{C_1E} (u_{C_1} - u_E) + (\gamma - 1)[Q]_{C_1E}\, \Delta t = 0, \tag{14a}$$

$$x_{C_1} - x_E = [u + c]_{C_1E}\, \Delta t; \tag{14b}$$

along C_1C_0 are

$$(1-\gamma)(P_{C_1}-P_{C_0})+2\gamma\left[\frac{P}{c}\right]_{C_1C_0}(c_{C_1}-c_{C_0})+(\gamma-1)[Q]_{C_1C_0}\,\Delta t=0, \quad (15a)$$

$$x_{C_1}-x_{C_0}=[u]_{C_1C_0}\,\Delta t. \quad (15b)$$

If we assume values for the terms in square brackets appropriate to the initial point on the base line from which the characteristics are drawn, then we can proceed in the following manner:

(1) Solve Eq. (15b) for x_{C_1}, the new position of the contact plane at time $t = t_1$.

(2) Solve

$$(u-c)_G=\frac{x_G-x_{C_0}}{x_A-x_{C_0}}(u-c)_A+\frac{x_G-x_A}{x_{C_0}-x_A}(u-c)_{C_0},$$

$$(u+c)_E=\frac{x_E-x_{C_0}}{x_D-x_{C_0}}(u+c)_D+\frac{x_E-x_D}{x_{C_0}-x_D}(u+c)_{C_0},$$

together with Eqs. (13b) and (14b) for x_G, x_E. The conditions at A, D, and C_0 are are assumed to be known.

(3) Interpolate conditions at the points G and E between the values at A, C_0, and D.

(4) Solve Eqs. (13a) and (14a) for u_{C_1} and P_{C_1}.

(5) Solve Eq. (15a) for c_{C_1}.

(6) The terms in square brackets may now be recalculated as the average of the values at the points C_0 and C_1, and the process repeated from (1) until all quantities have converged.

In general the pressure and velocity are continuous across a contact surface; the temperature and density are not. At the contact surface we, therefore, have four unknowns, the continuous pressure and velocity and the two values of the sound speeds—c_L to the left, and c_R to the right of the contact surface. We, therefore, must introduce two points at the contact surface, one each for the fluid immediately to the left and to the right of the contact plane. Equations (13) and (14) are then applied on the left point using c_L, while Eq. (14) and (15) are used with c_R on the right point. The four equations may then be solved for P_{C_1}, u_{C_1}, C_L, C_R. In our problem both gas 1 and 2 are assumed to have the same physical properties; thus, the temperature (and, hence, the sound speed) is also continuous across the contact plane if we start with an equal temperature across it. We, therefore, do not

need to introduce two points at the contact surface and to use c_L on the left point and c_R on the right point.

D. *Interpolation of an Additional Point Near the Shock*

Referring to Fig. 5 the conditions at points S_0, A, etc. on the line t_0 are given from previous computations. The determination of the point nearest to the shock front requires special study.

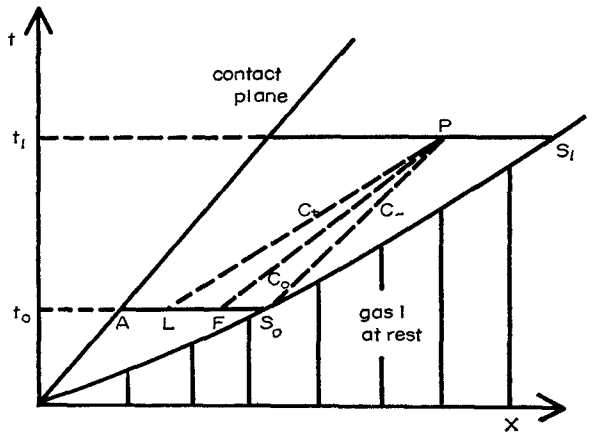

FIG. 5. Calculation of the point nearest to the shock.

We first draw a (negative) characteristic from S_0 to intersect the horizontal line t_1 at point P, and trace back next from point P two characteristics, one meets the base line t_0 at F(i.e., a streamline through point F), while the other intersects the base line t_0 at L.

The difference equations to be solved along PS_0 are

$$(P_P - P_{S_0}) - \gamma \left[\frac{P}{c}\right]_{PS_0} (u_P - u_{S_0}) + (\gamma - 1)[Q]_{PS_0} \Delta t = 0, \tag{16a}$$

$$x_P - x_{S_0} = [u - c]_{PS_0} \Delta t; \tag{16b}$$

along PL are

$$(P_P - P_L) + \gamma \left[\frac{P}{c}\right]_{PL} (u_P - u_L) + (\gamma - 1)[Q]_{PL} \Delta t = 0, \tag{17a}$$

$$x_P - x_L = [u + c]_{PL} \Delta t; \tag{17b}$$

along PF are

$$(1 - \gamma)(P_P - P_F) + 2\gamma \left[\frac{P}{c}\right]_{PF} (c_P - c_F) + (\gamma - 1)[Q]_{PF}\, \Delta t = 0, \quad (18a)$$

$$x_P - x_F = [u]_{PF}\, \Delta t. \quad (18b)$$

We first assume values for the terms in square brackets appropriate to the initial points on the base line from which the characteristics are drawn, and then proceeds as follows:

(1) Solve Eq. (16b) for x_p, the position of the point nearest to the schock.

(2) Solve the following four equations simultaneously for x_L, x_F, $(u - c)_L$, and $(u)_P$:

$$(u + c)_L = (u + c)_{S_0} \frac{x_L - x_A}{x_{S_0} - x_A} + (u + c)_A \frac{x_L - x_{S_0}}{x_A - x_{S_0}},$$

$$(u)_F = (u)_{S_0} \frac{x_F - x_A}{x_{S_0} - x_A} + (u)_A \frac{x_F - x_{S_0}}{x_A - x_{S_0}},$$

with Eqs. (17b) and (18b).

(3) Interpolate conditions at the points F and L between the values at points S_0, A.

(4) Solve Eqs. (16a) and (17a) for u_P and P_P.

(5) Solve Eq. (18a) for c_P.

(6) The terms in square brackets may now be calculated as the average of the values at the points P, L, F, and S_0, and the process repeated from (1) until all quantities have converged.

E. *Determination of the Time Step*

In the calculation of new points by characteristics at fixed time interval, we have to define the time step first. Referring to Fig. 6, in order to avoid a situation in which a characteristic would intersect a shock world line between time steps, we draw two characteristics from points S_0 and A (first tabular point behind shock S_0) intersecting at P. The following equation hold to a first order approximation

$$x_P - x_{S_0} = (u - c)_{S_0}\, \Delta t, \quad (19)$$

along PS_0, and

$$x_P - x_A = (u + c)_A\, \Delta t, \quad (20)$$

along PA.

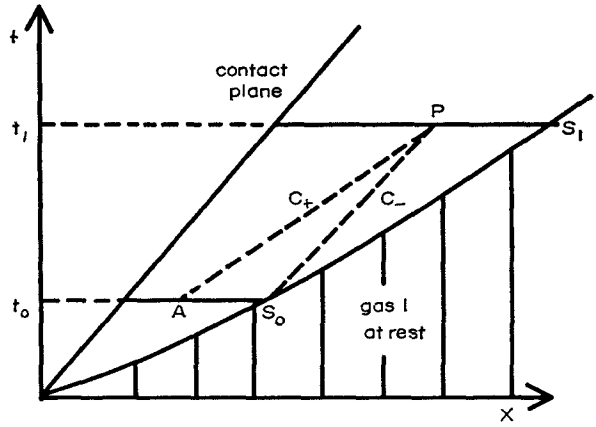

FIG. 6. Determination of the time step.

Solving Eqs. (19) and (20) yields

$$t = \frac{x_{S_0} - x_A}{(u + c)_A - (u - c)_{S_0}}, \tag{21}$$

since we have two shocks spreading out in our problems we will call Δt_1 and Δt_2 the time calculated for gas 1 and gas 2, respectively. Let $\Delta t_{\min}$ denote the smaller of Δt_1 and Δt_2, and Δt_{fix} the fixed time interval chosen in advance. If $\Delta t_{\min}$ is smaller than Δt_{fix}, we set the time interval $\Delta t = \Delta t_{\text{fix}}$ and go through the computations from Section A to Section C, but discard Section D; on the other hand if $\Delta t_{\min}$ is greater than Δt_{fix}, we set $\Delta t = \text{const} \times \Delta t_{\min}$ and go through all computations from Section A to Section D, i.e., we generate a new point next to the shock point S_1 at this time. The constant (the ratio $\Delta t/\Delta t_{\min}$) is used to control the number of points.

We futher use Courant stability condition to limit time step and to maintain stability. Since our method is essentially Lagrangian, this means that we must have

$$\Delta t < \Delta x/C,$$

where Δx is the interval over which the interpolation is performed.

IV. An Example — High-Velocity Cloud Collisions

We calculated the consequences when high momentum extragalactic clouds collide with galactic gases; the extragalactic gases having initial velocities of about 500 km/sec with respect to local standard of rest [6]. After collision, two strong

radiative shocks appear and move away from the contact surface into galactic and extragalactic gases, respectively. The calculations were done for an initial density ratio ρ_1/ρ_2 of unity at $t = 0$ (i.e., with equal densities in the galactic and extragalactic gases at collision) under the following physical conditions or restrictions:

(1) The extragalactic cloud is taken to be homogeneous, and the galactic gas density, n_H, is represented by:

$$n_H = n_0 \exp(-z/q_0) \text{ H-atoms/cm}^3,$$

where z is measured in parsec above the galactic plane, and the scale height $q_0 = 120$ parsec, $n_0 = 0.7$ H-atoms/cm^3.

This layer ends at about $z = 600$ parsec, beyond which lies the corona. The shocks are assumed to begin at this height.

(2) The radiation loss rates are taken from Pottasch (1965), with H, He, O, C, Mg, Si, and Ne abundances of $1 : 10^{-1} : 10^{-3} : 10^{-3.3} : 10^{-4} : 10^{-4} : 10^{-4}$ and ionization equilibria according to [5]. Although hydrogen and helium dominate in abundances, the energy losses are mainly caused by collisional transitions in the heavier ions.

(3) Both the preshock and the postshock gases are taken to be perfect gases:

$$P = \frac{K\rho}{\mu H} T, \qquad P' = \frac{K\rho'}{\mu' H} T'.$$

The notations are the usual, μ and μ' denote mean particle mass expressed in the units of the mass of proton.

The postshock gas is a rarefied plasma, in which the density is still low and the mean free path of the particles is very large, so that the mean energy of the Coulomb interaction between neighboring particles is small in comparison with the mean thermal energy of the particles and we can neglect it; thus, the postshock gas can be considered as a perfect gas.

(4) The precursor effects upon the preshock state are neglected, and these uniform conditions ahead of the shock front are adopted: the density, pressure and temperature take unperturbed values, and in particular, both gases are taken to be originally at temperature of about 100 K.

(5) Values of the ionization parameters are taken from Savedoff (1967):

$$\mu_1 = \mu_2 = 1.273, \quad \mu_1' = \mu_2' = 0.625, \quad \mu_e = 1.2, \qquad \text{and} \qquad V_i = 50 \text{ km/sec},$$

where $\frac{1}{2}V_i^2$ represents the ionization energy per gram. Values of some initial param-

eters connected with the two shocks created by a gas collision at relative velocity of about 500 km/sec are also taken from [8]:

$$\rho_1/\rho_1' = 0.242, \qquad S_1 = 330 \text{ km/sec}, \qquad S_2 = 170 \text{ km/sec},$$
$$T_1' = T_2' = 1.52 \times 10^6 \text{ K},$$

where S_1 and S_2 are the galactic shock velocity and the cloud shock velocity relative to the galactic gas, respectively. We work in a coordinate system in which the galactic gas is at rest and the extragalactic gas approaches it with a velocity of

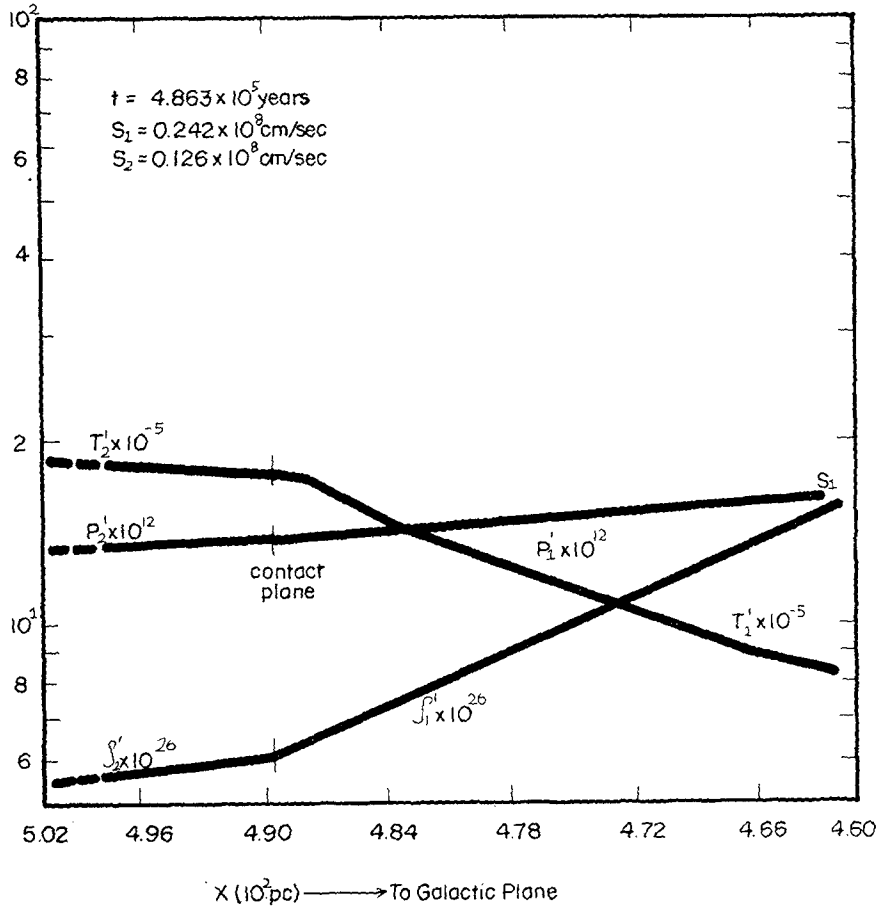

FIG. 7. Spatial temperature, pressure, and density profiles for the gases behind shocks at $t = 4.863 \times 10^6$ yr.

about 500 km/sec. Index 1 is reserved for galactic gas and index 2, for extragalactic gas.

The results have been given in detail by [1]. We summarize them in the following manner.

At first the spatial temperature profile increases smoothly from the galactic shock front to the cloud shock front, the negative temperature gradient becoming more negative with increasing time. The pressure and density profiles decreasing smoothly from the galactic shock front to the cloud shock front, although the

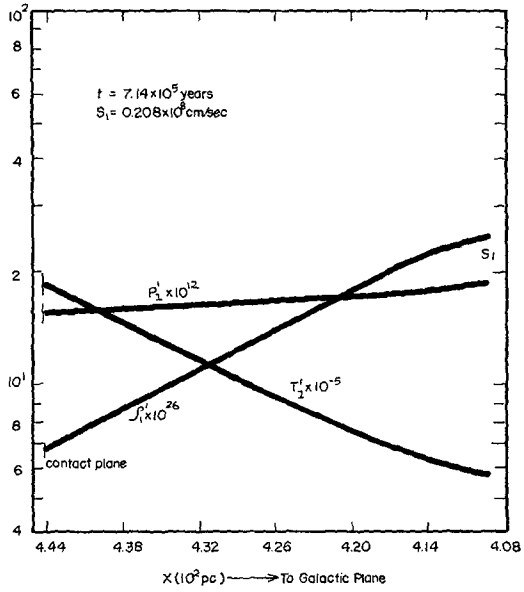

FIG. 8. Spatial temperature pressure, and density profiles for the gases behind the galactic shock at $t = 7.14 \times 10^5$ yr. Temperature inversion begins to develop.

absolute density and pressure increase slightly with increasing time. This temporal increase gradually slows after about 7×10^5 years (at this age, $T_1 = 5.8 \times 10^5$ K), when there also appears on the galactic side a "depression" in the initial smooth temperature and pressure profiles as shown in Figs. 7–9. Subsequently, this "depression" acquires the form of a "deep-well" as shown in Fig. 10. Figure 11 shows the development of the pressure dip.

This differs from those derived from steady state solutions, which predicts that these dips should appear first at the contact surface. These previous treatments neglect the change in the flow pattern caused by the cooling contraction of the

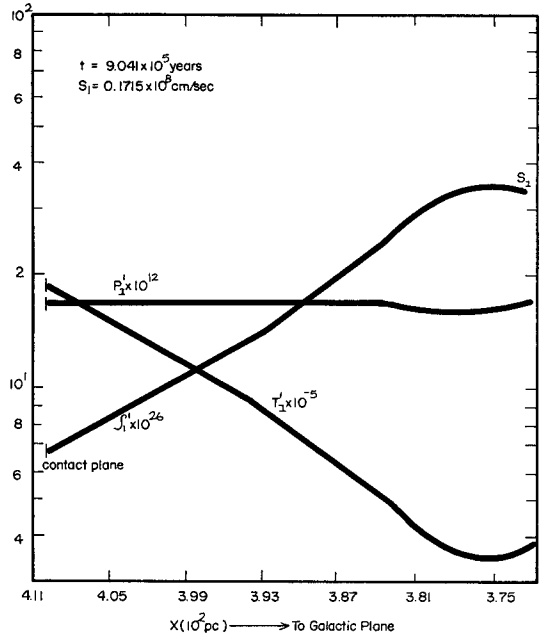

FIG. 9. Spatial temperature, pressure, and density profiles for the gases behind the galactic shock at $t = 9.041 \times 10^5$ yr.

postshock gas. The cooling causes the shocks to slow down with respect to the gas they are penetrating, and this gives rise to complications behind the shock fronts describable as compression and expansion waves. For shocks in colliding non-homogeneous gas clouds, the complications behind the shock fronts are far greater, because of both the cooling contraction of the postshock gas and the effects of external density and pressure variations upon the shock propagation. The detail discussion can be found in the paper by Chow and Savedoff [1]. A quantitative condition for the growth of the dips follows on considering perturbations of the flow. We consider a small perturbation $\delta u'$, $\delta p'$, $\delta \rho'$, etc. on a desired solution $u'(x, t)$, $p'(x, t)$ etc. and investigate whether the perturbation grows with increasing time [9]. To do this we replace u' etc. by $u' + \delta u'$ etc. in Eqs. (1)–(3) and get a set of three simultaneous linear differential equations for $\delta u'$, $\delta p'$, etc. Their coefficients depend on the desired solutions u', p', etc. We treat these coefficients as constants in a small region and look for solutions of the form $\delta u' = \delta u_0 \exp(\alpha t + ikx),)$etc., where u_0, etc., and k, α are constants and k is real. Substitution of these into the simultaneous linear differential equations for $\delta u'$, $\delta p'$, etc. leads to three simultaneous homogeneous linear equations in δu_0,

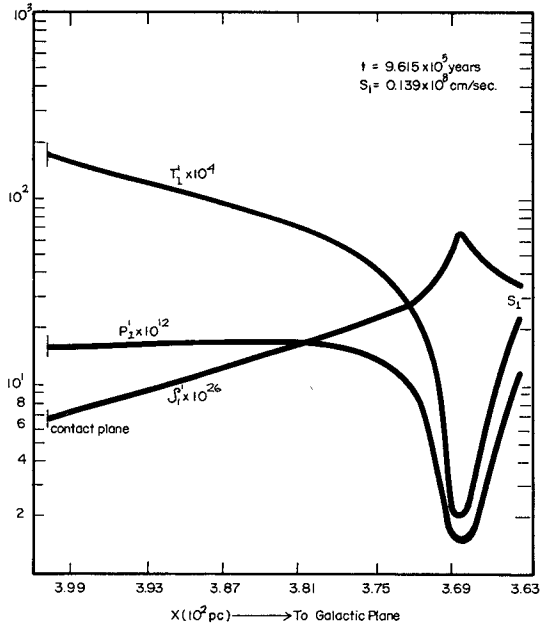

FIG. 10. Spatial temperature, pressure, and density profiles for the gases behind the galactic shock at $t = 9.615 \times 10^5$ yr. The gas at the dip has cooled to 20,000 K.

δp_0, etc. The vanishing of the determinant of these equations yields an equation connecting k and α. By solving this equation for α with a given k, we can determine whether a given Fourier component of the perturbation $\delta u' = \delta u_0 \exp(\alpha t + ikx)$ etc. grows with increasing time. The real part of the sum of the three roots of α is independent of k and satisfies

$$\mathrm{Re}(\Sigma\alpha) \geqslant \frac{1}{\rho'}\left[\frac{(\gamma+2)}{3}\frac{d\rho'}{dt} - \frac{\gamma-1}{3R}\left(\frac{\partial Q}{\partial T'}\right)_{\rho'}\right].$$

It is seen that if $\mathrm{Re}(\Sigma\alpha) > 0$, then there exists at least one root with $\alpha > 0$. Hence, during compression the system is unstable, and the growth of the dips is formed both by the compression and the energy loss term for $T' > 3 \times 10^5$ K (for $T' > 3 \times 10^5$ K, $(\partial Q/\partial T')_\rho < 0$, [5]). For lower temperature, $(\partial Q/\partial T')_\rho > 0$, hence $\mathrm{Re}(\Sigma\alpha)$ may be negative, but we can not find any useful upper limit on α because of algebraic complexity. In our calculations which end at 2×10^4 K, it takes only three steps (of 5000 years per step) to evolve from 2×10^5 K to 2×10^4 K. It is desirable to repeat this part calculations with small time intervals to better determine the evolution of the dips when radiation losses decreases with decreasing temperature.

The reliability of our calculations has been examined by checking the consistency with the following conservation laws:

Mass conservation

$$\rho_1 x_1(1) = \int_{x_c}^{x_1(1)} \rho_1'(x)\, dx,$$

where x_c denotes the position of the contact surface. This relation says that the total mass within the post-shock region is equal to the total mass swept by the shock.

Energy conservation

$$\int_{t_1}^{t_2} (p_1' u_1')_c\, dt + \int_{t_1} (\tfrac{3}{2} p_1' + \tfrac{1}{2}\rho_1' u_1'^2 + \tfrac{1}{2}\rho_1' V_i^2)\, dx - \int_{t_2} (\tfrac{3}{2} p_1' + \tfrac{1}{2} p_1' u_1'^2 + \tfrac{1}{2}\rho_1' V_i^2)\, dx = \iint Q\, dx\, dt,$$

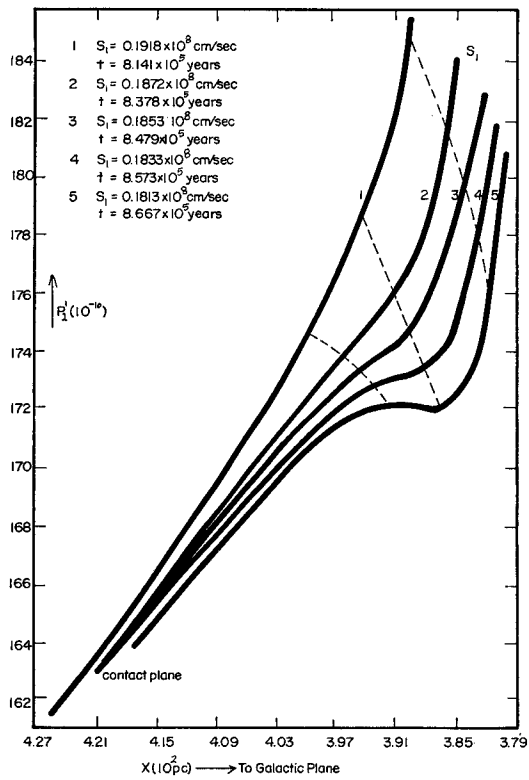

FIG. 11. The development of the pressure dips.

where t_1 and t_2 written at the bottom of the integral signs means that the integrals are evaluated at times t_1 and t_2, respectively, and $(Pu)_c$ means that Pu is evaluated at the contact surface.

Momentum conservation

$$\int_{t_1}^{t_2} (p_1')_c \, dt = \int_{t_2} \rho_1' u_1' \, dx - \int_{t_1} \rho_1' u_1' \, dx.$$

The computations for the galactic shock from $t_1 = 7.14 \times 10^5$ yr to $t_2 = 9.467 \times 10^5$ yr gave

$$\frac{\Delta(\text{mass})}{\rho_1 x_1(1)} = 6.7 \times 10^{-5}, \qquad \frac{\Delta(\text{momentum})}{\int_{t_1}^{t'} (p_1')_c \, dt} = 5.5 \times 10^{-4}$$

and

$$\frac{\Delta(\text{energy})}{\int_{t_1}^{t'} (p_1' u_1')_c \, dt} = 1.4 \times 10^{-2},$$

where Δ (mass) denote the difference over the right and the left sides of the mass conservation equation. This integral test indicates that there is no large systematic errors in our programs.

Acknowledgment

It is a pleasure to thank an anonymous referee for many pertinent comments.

References

1. T. L. Chow and M. P. Savedoff, *Nuovo Cimento* **8B** (1972), 130–142.
2. R. Courant and K. Friedricks, "Supersonic Flow and Shock Waves," Wiley, New York, 1948.
3. D. R. Hartree, 1953, AECU-2713.
4. N. E. Hoskin, "Methods in Computational Physics," Vol. 3, Academic Press, New York, 1965.
5. L. House, *Astrophys. J. Suppl.* (1964), 307.
6. J. H. Orrt, Preprints, 1965.
7. S. R. Pottasch, *Bull. Astro. Inst. Netherlands*, **18** (1965), 7.
8. M. P. Savedoff, J. W. Hovenier, and B. Van Leer, *Bull. Astro. Inst. Netherlands* **19** (1967), 107.
9. J. Von Neumann and R. D. Richtmyer, *J. Appl. Phys.* **21** (1950), 232.